CF3I Gas and its Mixtures

21, rue d'Artois, F-75008 PARIS
http : //www.cigre.org

D1-308

CIGRE 2014

CF_3I Gas and Its Mixtures: Potential for Electrical Insulation

M. S. KAMARUDIN, L. CHEN*, P. WIDGER, K. H. ELNADDAB, M. ALBANO, H. GRIFFITHS AND A. HADDAD,
Advance High Voltage Engineering Research Centre, Cardiff University
United Kingdom

SUMMARY

SF_6 is a potent greenhouse gas with a global warming potential (GWP) of 23,900 times that of CO_2 and atmospheric lifetime exceeding 1000 years. For this reason, there has been research into alternative insulation gases with the aim of reduced SF_6 gas content in high-voltage equipment. The research, so far, into alternative gases has shown that CF_3I and its gas mixtures have promising dielectric properties comparable to those of SF_6. This paper provides an overview of research into alternative gases to SF_6. These include laboratory tests on the gases and initial applications to electrical power equipment.

In this work, the dielectric strength of CF_3I and its mixtures with CO_2 was experimentally examined under lightning impulse conditions. To investigate the properties of CF_3I, a steel cylindrical pressure vessel has been built with a pair of brass electrodes inside. Uniform and non-uniform field behaviour was generated by using different electrode arrangements. Tests were carried out on gas mixtures of CF_3I-CO_2 (in particular 30:70%) at 0.1 MPa (abs). It was found that, for various gap geometries (rod-plane and plane-plane electrodes) and lengths, CF_3I mixtures exhibit promising breakdown characteristics comparable to those of SF_6 gas based on the measured 50% breakdown voltage (U_{50}). These encouraging results led to a trial of CF_3I as the insulation gas on practical 11 kV low-current switches and circuit breakers. In particular, a Ring Main Unit (RMU) was tested to compare the performance of 30:70% CF_3I-CO_2 mixture with 100% SF_6 when subjected to the rated lightning impulse withstand voltage (U_p). This work demonstrated the feasibility of replacing SF_6 with the new gas mixture without the need to modify the geometry of the switchgear. However, research has shown that interruption of arc currents is rather limited to up to about 100 A [1]; beyond this level further research is required.

The fundamental laboratory experiments on the new gas were extended to coaxial geometries replicating electric field magnitudes (160-200 kV/cm) as found in a 400 kV GIS/GIL under lightning voltage impulse of 1425 kV. The ultimate aim of this work on coaxial models is the feasibility of GIL using CF_3I mixtures which is investigated in a parallel project. An EMTP-ATP model has been developed to study the characteristics of GIL as a long transmission system. Steady state results obtained suggest that reactive power compensation is not required for up to 300 km. Simulation results show that GIL using CF_3I gas mixtures may provide an attractive alternative to long cable and overhead lines.

KEYWORDS

Gas Insulated Lines (GIL), Gas Insulated Switchgear (GIS), Trifluoroiodomethane (CF_3I), Sulfur Hexafluoride (SF_6).

*Co-ordinating author's email address: chent3@cardiff.ac.uk

1. Introduction

SF_6 is an electronegative gas and it has dielectric strength three times higher than air. The outstanding properties of SF_6 have resulted in its extensive use as an insulation gas in high-voltage equipment. On the other hand, it is a highly potent greenhouse gas due to its high global warming potential, around 23,900 times that of CO_2. Alternatives insulation gases to replace SF_6 have been investigated in recent decades and one emerging candidate is CF_3I gas. SF_6 and CF_3I have a number of similar properties: both gases are colourless， odourless and non-flammable. The weak chemical bond C-I in CF_3I means that it can be decomposed quickly in the atmosphere, and therefore the ozone depletion potential of CF_3I for surface release is less than 0.0001 [2]. In this way, CF_3I is considered to be an environmentally friendly replacement to SF_6. However, CF_3I has a high boiling point of –22.5°C at atmospheric pressure, as reported in [3]. This makes the use of pure CF_3I less applicable for HV GIS/GIL equipment, which is normally pressurised at above 0.5 MPa. When considering CF_3I as an alternative to SF_6, it is important to take into account that switchgear operated on the MV (11 kV) network uses SF_6 at a very low pressure (just above atmospheric pressure). For this reason, CF_3I could be considered as a potential replacement candidate.

This paper provides an overview of the research work that has been conducted on CF_3I gas at Cardiff University. In the paper, we present the results of the experimental investigations carried out on CF_3I-CO_2 mixtures of 30:70% including a) a comparison of properties between SF_6 and CF_3I mixture, b) breakdown results obtained on rod-plane and plane-plane configurations filled with CF_3I-CO_2 mixtures; c) laboratory performance results of industrial switchgear designed for SF_6 gas when the gas is replaced with CF_3I mixtures; d) a new scaled coaxial test rig to explore dielectric properties of gas insulated lines (GIL) using CF_3I gas, and e) power systems studies investigating the performance of CF_3I GIL for long distance transmission.

2. Comparison of Properties of SF_6 and CF_3I Mixtures

Partial pressure of CF_3I in the mixture is selected by a trade-off between three basic factors; boiling point of the gas mixture, insulation strength, and the by-products of the gas mixture upon each electrical discharge.

2.1 Saturation Vapour Pressure

Typically, in a GIL system, SF_6 gas is pressurised at 0.7 MPa. It can be seen from Figure 1 that the boiling point of CF_3I at 0.7 MPa is 38°C, an indication that a buffer gas such as carbon dioxide (CO_2) needs to be added to CF_3I in order to reduce the boiling temperature.

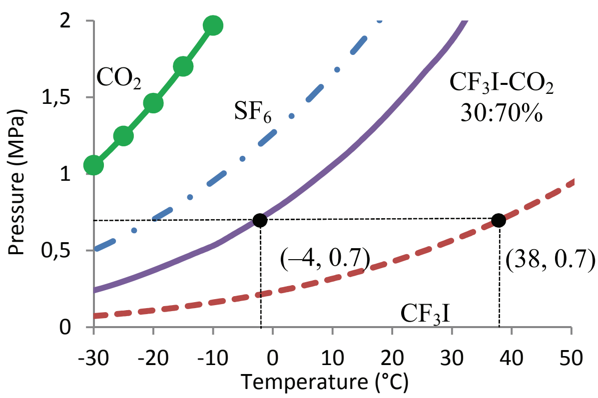

Figure 1 : Saturation vapour pressure curve of SF_6, CF_3I, CO_2 and 30:70% CF_3I-CO_2 mixture.

2.2 Ionisation Coefficients

Effective ionisation coefficients of different gases and gas mixtures were computed using Bolsig+ software which applies the two-term approximation of Boltzmann equation [4]. Figure 2 shows the pressure-reduced ionisation coefficient $(\alpha - \eta) / p$ as a function of E / p for different pure gases and CF_3I mixtures. It can be seen from Figure 2 that the critical reduced field strength at which $(\alpha - \eta) = 0$ for CF_3I is 108 kV/cm bar compared to 89 kV/cm bar in SF_6 [5]. This is consistent with results reported in [6] which indicate that pure CF_3I has a dielectric strength of around 1.2 times higher than that SF_6.

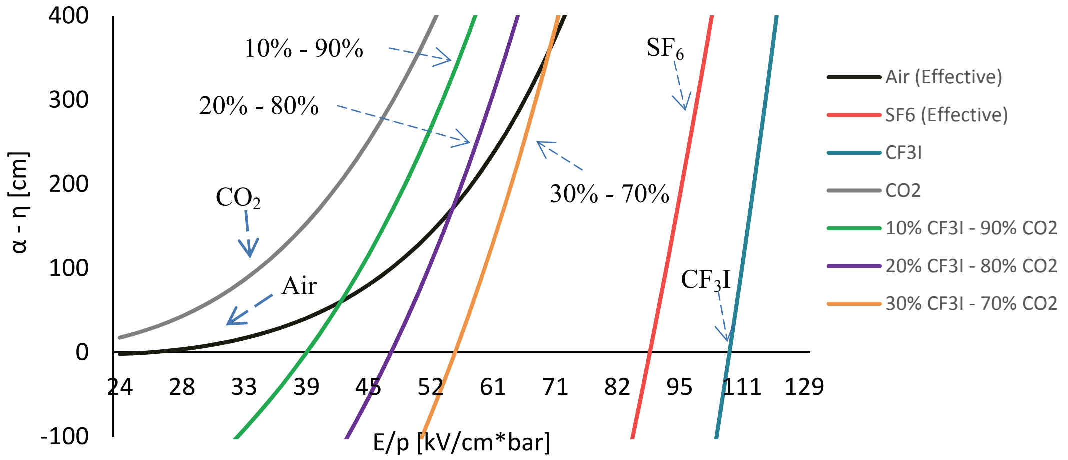

Figure 2: Effective ionisation coefficients in pure gases (Air, SF_6, CF_3I and CO_2) and CF_3I-CO_2 mixtures (10%-90%, 20%-80% and 30:70%)

Figure 2 shows that 30:70% mixture ratio has a higher reduced field strength E/p compared to CF_3I-CO_2 mixtures with low CF_3I contents. The 30:70% mixture ratio is considered to be most appropriate for gas-insulated switchgear (GIS) applications according to Katagiri et al. [7]. Kasuya et al. [8] suggested the same ratio for gas circuit breaker (GCB) applications. According to Katagiri et al. [7], for the same ratio, the interruption capability of CF_3I-CO_2 mixtures is far superior to that of CF_3I-N_2 mixtures. With only 30% of CF_3I in the CF_3I-CO_2 mixture, the insulation performance was reported to be approximately 0.75 to 0.80 times that of SF_6. The 30:70% mixture ratio, therefore, offers a reasonably high dielectric strength while been able to sustain its gaseous form at 0.7 MPa with a boiling temperature of mixture of around –4°C. Furthermore, by-products produced during arcing such as iodine can be reduced substantially using 30:70% mixture, which is indicated in another paper by Kasuya et al. [1]. It is important to minimise iodine deposition as it can compromise CF_3I insulation performance, as reported by Takeda et al. [9].

3. Breakdown Strength under Rod-plane and Plane-plane Configurations

To characterise the 30:70% CF_3I-CO_2 mixture as an insulation medium, lightning impulse experiments with both polarities were conducted on two electrode configurations, as shown in Figure 3. The up and down method [10] was used to determine the 50% breakdown voltage (U_{50}), and using this value, simulations were carried out using COMSOL to obtain the equivalent maximum electric field (E_{max}) at the breakdown voltage.

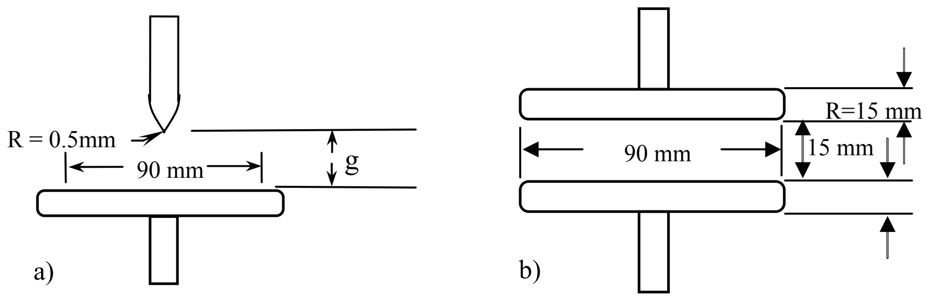

Figure 3: a) Rod-plane and b) Plane-plane electrode configurations

The field utilisation factor, η, was calculated using Equation (1). This is expressed as an approximate index of field uniformity of the electrode geometry, where a higher field utilisation factor represents a more uniform electric field configuration. 'g' represents the gap length between the HV and earth electrodes.

$$\eta = \frac{E_{mean}}{E_{max}} \tag{1}$$

Where

$$E_{mean} = \frac{U_{50}}{g} \tag{2}$$

3.1 Rod-plane Electrode Configuration

In this test, a rod-plane electrode configuration has been chosen to represent very non-uniform electric field behaviour as shown in Figure 3a, and the results are shown in Figure 4. For a 1 cm gap, the U_{50} of the CF_3I gas mixture is the same for both lightning impulse polarities. When the gap length is increased, U_{50} for both impulse polarities also increases. The field utilisation factor, however, decreases as the gap length is increased which indicates higher non-uniformity. Under negative impulse, the increment in U_{50} is more significant compared to that under positive impulse. At 5 cm and under negative impulse, U_{50} has increased to almost 3 times compared with U_{50} at 1 cm. Meanwhile, under positive impulse, the increment is about 1.8 times.

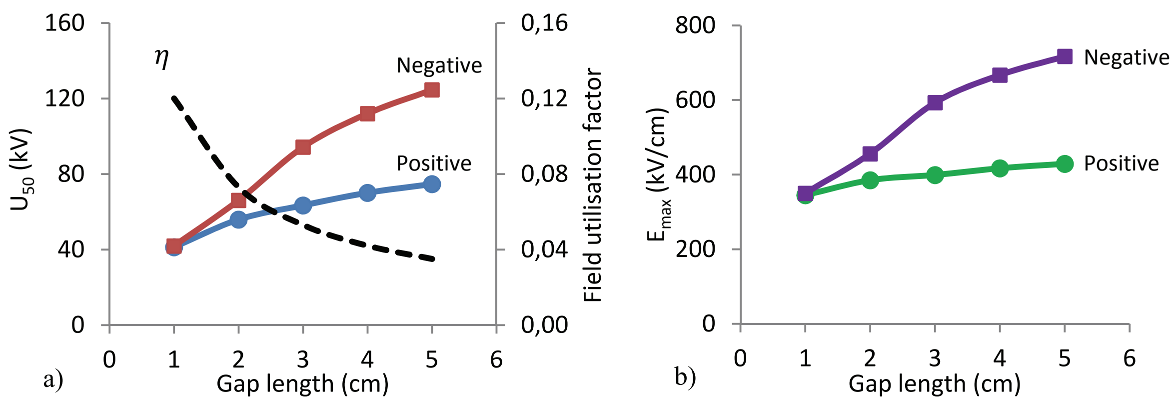

Figure 4: U_{50} and E_{max} curve for 30:70% CF_3I-CO_2 gas mixture in a rod-plane electrode configuration under positive and negative lightning impulses

Generally, it can be said that for the rod-plane electrode configuration, the U_{50} voltage under a negative impulse voltage is higher than U_{50} under a positive impulse voltage, similar to observations in air gaps. As discussed by Loeb and Kip [11], breakdown in the rod-plane electrode is due to the streamers. In negative streamers, the space charge build-up impedes the negative avalanche, while the space charge in positive streamers propagates toward the cathode. Due to this process, negative streamers require higher electric fields (and therefore higher breakdown voltages) than positive streamers [12] to obtain full breakdown of the gap.

3.2 Plane-plane Electrode Configuration

In the plane-plane electrode configuration shown in Figure 3b, it is expected that higher voltages are required in order for the CF_3I-CO_2 gas mixtures to achieve breakdown, when compared to a similar gap length configuration of the rod-plane configuration. It was essential, therefore, to limit the gap length such that the applied voltage is restricted for the safety of HV bushing in the experimental setup. For this reason, the gap length in this test is limited to 3 cm. Results for U_{50} and E_{max} under positive and negative impulse are plotted in relation to gap length, as shown in Figure 5.

The results in Figure 5 show a behaviour that is opposite from which was observed in the rod-plane configuration. In this plane-plane configuration, U_{50} under positive impulse is higher than under negative impulse. With a 1 cm gap, there is only a 3% difference between both polarities, and the observed voltage difference increases with gap length, 12.7% and 29% for 2 cm and 3 cm gaps respectively. Also, in this study, U_{50} can be seen to increase quite linearly with gap length in a plane-plane configuration, up to 3 cm. Under positive impulse, U_{50} increased to 2.8 times from a 1 cm gap to a 3 cm gap, and under negative impulse, the increment is approximately 2.4 times.

The trends in U_{50} curves reflect the behaviour in E_{max} curves, as can be seen in Figure 5. E_{max} is observed to increase linearly with gap length, although the increment is not as much as for U_{50}. For E_{max}, the increment from a 1 cm to 3 cm gap is 1.56 times that under a positive impulse and just 1.3 times under a negative impulse.

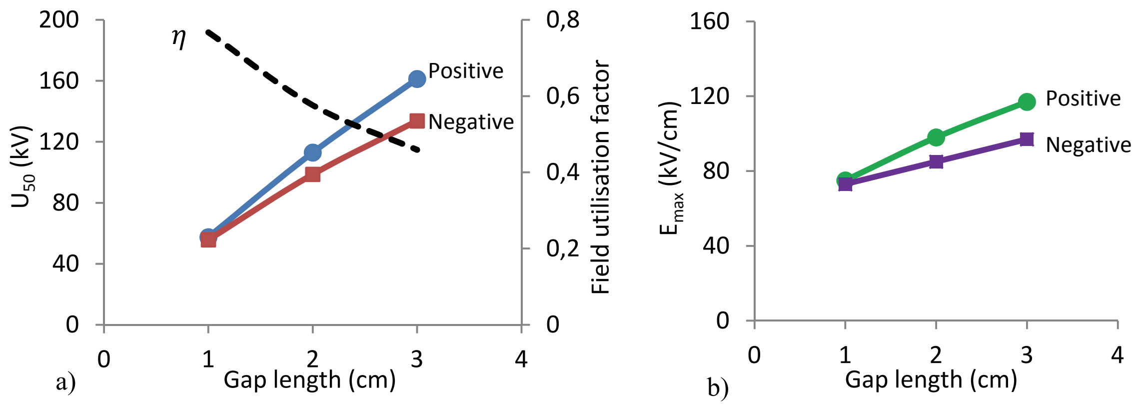

Figure 5: U_{50} and E_{max} curve for 30:70% CF_3I-CO_2 gas mixture in plane-plane electrode configuration under positive and negative lightning impulses

4. Switchgear Application

To trial the application of a 30:70% CF_3I-CO_2 mixture in switchgear, an existing commercial Ring Main Unit (RMU) normally filled with SF_6 was tested using the CF_3I mixture. The RMU comprises two low-current 'ring' switches and a tee-off vacuum circuit breaker contained within a common gas insulated chamber as shown in Figure 6. Figure 6a shows the test setup for one of the low-current switches while Figure 6b shows the test arrangement for the vacuum circuit breaker. A mixture of 30:70% CF_3I-CO_2 was used at the rated filling pressure of the RMU of 0.14 MPa (abs.) for all the tests.

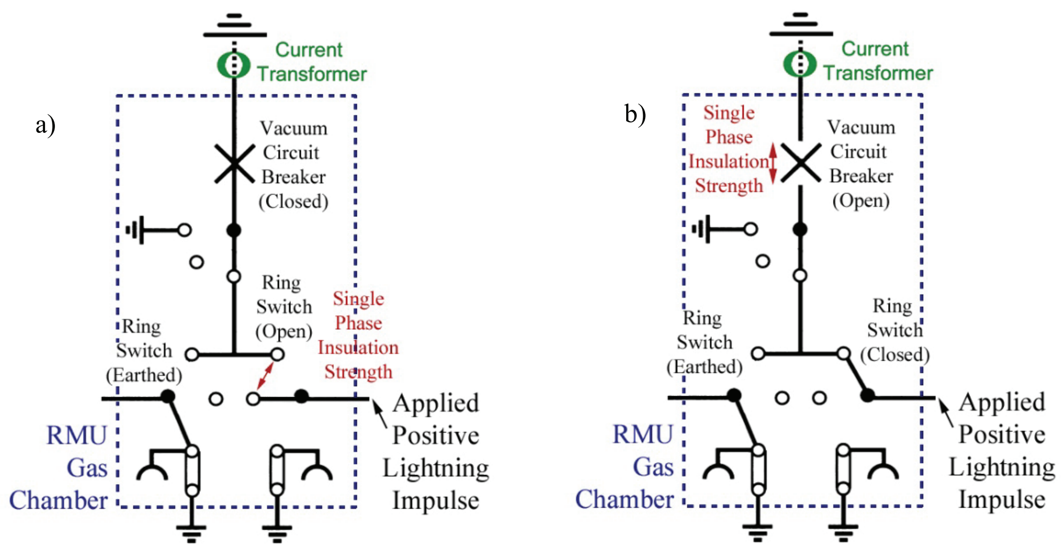

Figure 6: a) Test position for ring switch and b) test position for vacuum circuit breaker

The RMU filled with standard SF_6 gas has a rated impulse withstand voltage of 75 kV. The RMU was subjected to the withstand voltage test outlined in procedure B in BS60060-1, which has been adapted for switchgear and controlgear as set out in BS62271-1 [13] for impulse testing. Positive lightning impulses were applied to each phase in turn at a constant 75 kV. For the switches, one set of 25 impulses was applied to each phase to test the insulating withstand strength of the CF_3I-CO_2 gas mixture. For the vacuum circuit breakers, insulated by the CF_3I-CO_2 gas, two sets of impulses were applied to each phase of the RMU (a total of 50 impulses) to test the withstand strength of the gas mixture. The current transformer was used to identify a gas breakdown across the equipment.

The results of the test shown in Table 1 suggest that when the RMU is filled with an insulating gas mixture of 30:70% CF_3I-CO_2 no disruptive discharges are identified, either i) across the ring switch gas gap in a 25 impulse set or ii) across the vacuum circuit breaker in the 50 impulse set.

Table 1: 30:70% CF_3I-CO_2 RMU for 75 kV Positive Lightning Impulse Withstand Voltage tests

	Phase 1		**Phase 2**		**Phase 3**		**RMU Average**	
	Result	**No. of gas breakdowns**	**Result**	**No. of gas breakdowns**	**Result**	**No. of gas breakdowns**	**Result**	**No. of gas breakdowns**
Ring Switch	PASS	0/25	PASS	0/25	PASS	0/25	PASS	0/75
Circuit Breaker	PASS	0/50	PASS	0/50	PASS	0/50	PASS	0/150

The results in Table 1 suggest that the 30:70% CF_3I-CO_2 mixture can be a potential replacement for SF_6 in 11 kV switchgear. The current interruption capability of the 30:70% mixture has not been tested and, therefore, further work is required to establish whether the gas mixture could be used to insulate the ring switches.

5. Feasibility Study of GIL Using CF_3I Mixtures

The experiment using 30:70% CF_3I-CO_2 mixture described in Sections 3 and 4 show promising potential for gas insulation. Research using this same gas mixture was extended to a small-scale coaxial prototype system with the aim to explore the feasibility of replacing SF_6 in GIL/GIS systems.

5.1 Testing a Coaxial-GIL Model

The maximum electric field in a coaxial geometry is described by the following equation:

$$E_{max} = \frac{V_{applied}}{a\ \ln(\frac{b}{a})} \tag{3}$$

Where 'a' is the conductor radius and 'b' represents the inner enclosure radius.

For a typical 400kV GIL geometry [14] having an inner conductor of radius 9 cm and outer enclosure with inner radius 24 cm, the maximum electric field at the inner conductor surface when the maximum lightning withstand voltage level is applied is

$$E_{max} = \frac{1425\times 10^3}{9\times\ln(\frac{24}{9})} = 161.4\ \text{kV/cm} \tag{4}$$

To develop a laboratory scaled model, the design of the test geometry aimed to generate a similar maximum electric field within the voltage levels that can be applied to the test vessel. The selection of the dimensions 'a' and 'b' were based on practical constraints of fitting a small-scale coaxial system prototype inside the test vessel and voltage limitation of the HV bushing (approximately 85 kV). Another factor that need to be taken into consideration is the optimisation of the quantity log(b/a), for which a value of 1 is considered the optimal ratio [15] for gap distance and field uniformity inside a coaxial system. Using this approach, the nearest practical values of a and b were adopted giving a = 0.556 cm and b = 1.425 cm. Applying the dimensions of the scaled down coaxial system into Equation

(3), similar maximum electric field strength to that of the full GIL was achieved with a $V_{applied}$ of 85 kV. The dimensions of the small-scale coaxial system were then used to design a simulation model as shown in Figure 7. As can be seen from the figure, the middle section is an aluminium metal enclosure with an aluminium conductor inside. The two end insulators have circular shaped holes to allow gas circulation inside the test vessel.

$$E_{max} = \frac{85\times 10^3}{0.556\times\ln\left(\frac{1.425}{0.556}\right)} = 162.4\ \mathrm{kV/cm} \quad (5)$$

Detailed numerical simulations of the coaxial model were used to identify high electric stress regions. For the Coulomb simulations, the voltage on the conductor was set to 85 kV and the enclosure was grounded. As expected, the maximum electric field was found at the centre region of the conductor (E_{max} 163 kV/cm). There are also high electric field regions on the edges of the enclosure. These high stress regions were alleviated by adding two grading rings at the edges of the enclosure as shown in Figure 8.

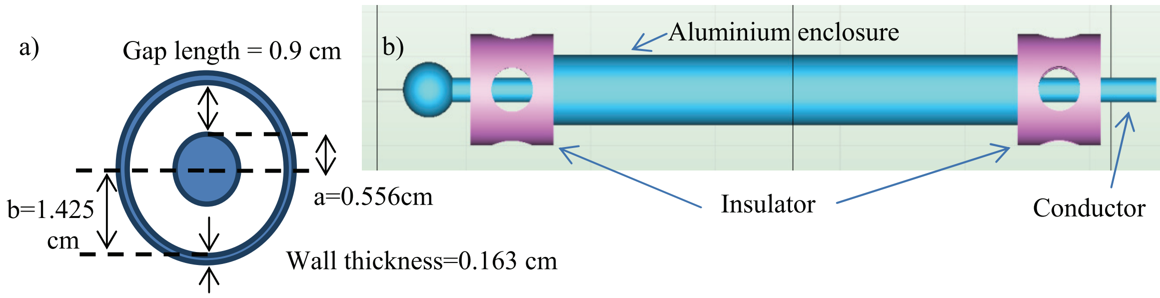

Figure 7: a) Dimensions of the coaxial model; b) side view of the coaxial model

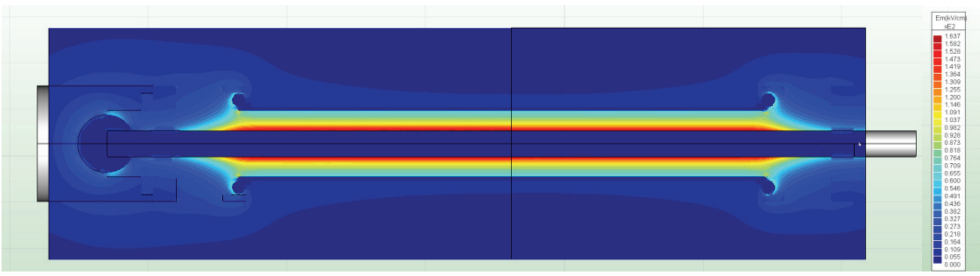

Figure 8: Computed distribution of electric field magnitude, where (E_{max} 163 kV/cm)

The refined fabricated model of the coaxial test system is shown in Figure 9a. The enclosure and conductor are both made out of aluminium metal, and a metal strip was welded onto one of the grading rings to make an earth connection. On the tip of the conductor there is 10 mm thread that is used for attaching the coaxial model onto a HV bushing inside the pressure vessel. The full setup of the experiment can be seen in Figure 9b. The lightning impulse was applied through the HV bushing and onto the test object. The up and down method was also used to determine U_{50} in this experiment. The tests were conducted with increasing pressure from 0.05 to 0.3 MPa (abs.).

The results are displayed in Figure 10 and, as expected, U_{50} increases against increasing pressure. At 0.2 MPa (abs.), the measured U_{50} is around 84 kV which is nearly the same as the terminal voltage of 85 kV that was initially calculated. Tests were also conducted for air at 0.2 MPa (abs.), and the measured U_{50} was 38 kV which makes 30:70% CF_3I-CO_2 mixture is 2.2 times higher than air under similar conditions. For a GIL system, it is important to minimise the occurrence of gas discharge. To do this, the withstand strength need be designed lower than the critical reduced field strength of whichever CF_3I mixture to be used as the insulation medium.

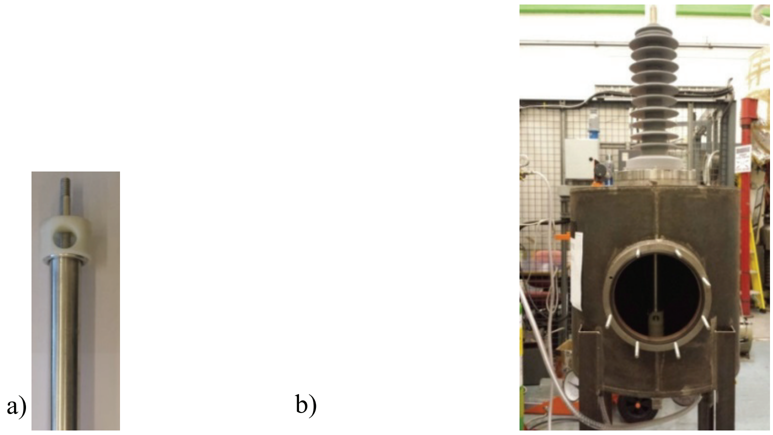

Figure 9: a) manufactured model; b) coaxial model set up inside the pressure vessel

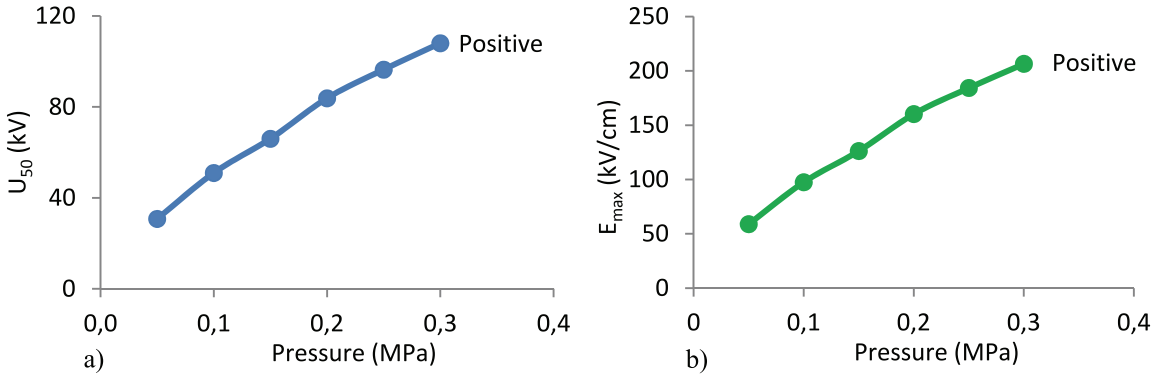

Figure 10: U_{50} and E_{max} curve for 30:70% CF_3I-CO_2 gas mixture in coaxial cylindrical geometry under positive lightning impulses as function of pressure.

5.2 Simulation Study of 400kV GIL System for Long Transmission of Bulk Power

An EMTP-ATP model shown in Figure 11 has been developed based on the geometric and the material properties of a typical 400 kV SF_6 GIL system [14] to study the characteristics of a GIL as a long transmission system. The purpose of this simulation is to determine the transmission capacity limit without reactive power compensation. The model is represented by three phase single core line and divided into six 50 km sections.

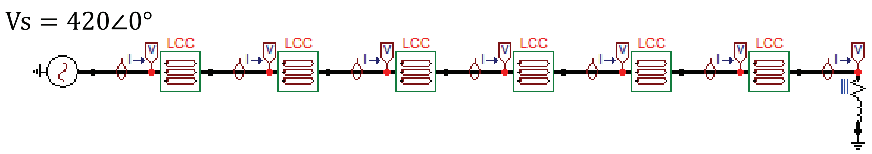

Figure 11: EMTP-ATP simulation model

In Figure 12a, according to [16] the voltage drop limit should be within ±5%. The simulation shows that this was reached at 800 km length and 90% of the transmitted power was reached at 670 km. This indicates a low power loss over long distance transmission for a GIL system. The maximum transmitted power versus line length can be limited by factors such as reactive power generated by the shunt capacitance, load condition and operation power factor. The power factor and load condition was set as 0.8 and 100%, respectively, which was achieved by load regulation at the receiving end. Voltage profiles for different line lengths, ranging from 200 to 500 km, are shown in Figure 12b. As can be seen, the voltage drop at 200 km is 11%, and this is increased to 23.5% at 500 km under full load conditions.

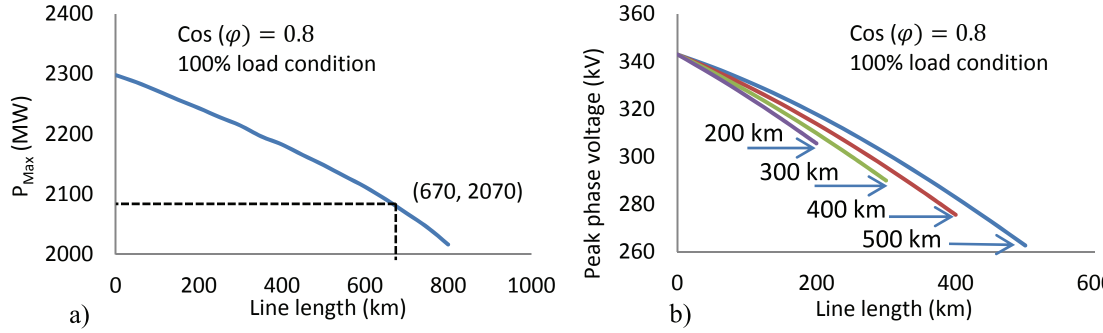

Figure 12: a) Maximum transmitted power against increasing distance; b) Voltage profiles for GIL from 200-500km.

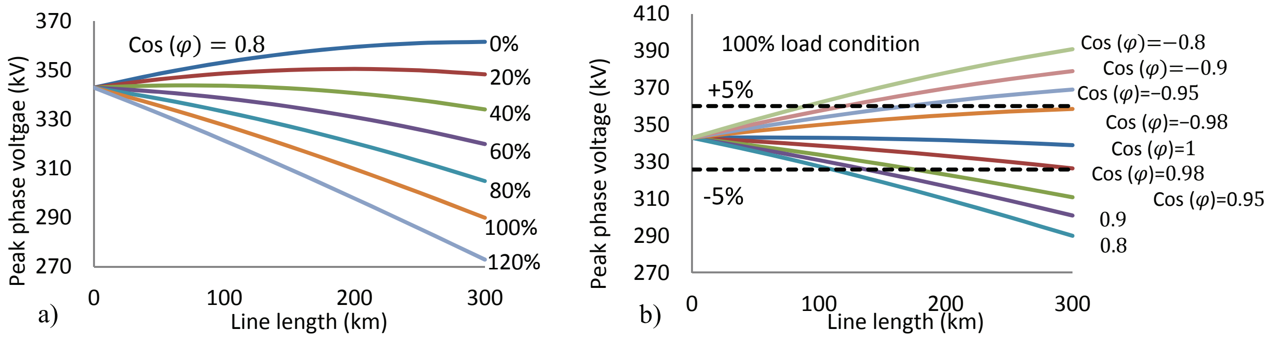

Figure 13: a) Voltage profiles under various load conditions and b) for different power factors.

Further simulations were conducted to analyse the change in voltage at different load conditions and power factors. For a line length of 300 km, load conditions ranging from 0% to 120% were studied using 0.8 power factor. The drop in voltage for 0% load condition is 5.44%, and this changed to –0.4% for 120% load condition, as shown in Figure 13a. It can be seen from Figure 13b that the power factor was adjusted to analyse the change in voltage profile with 100% load condition maintained. The voltage drop at unity power factor is –1.2%. When the power factor was adjusted from unity to 0.8 lagging, the voltage drop is increased to –15.45%. On the other hand, when the power factor was changed from unity to 0.8 leading, the voltage drop is around 14%. The simulation results show that utilizing GIL as a transmission system up to 300 km is possible with ±0.98 power factor and 100% load condition without reactive power compensation.

6. Conclusion

This paper discussed the work carried out on CF_3I mixture and its potential to replace SF_6 in high-voltage equipment. 50% breakdown tests conducted on three electrode configurations (rod-plane, plane-plane and coaxial) were used to characterise 30:70% mixture of CF_3I-CO_2. The breakdown strength of the mixture for coaxial electrode was more than two times higher than air. In comparison, breakdown strength of pure SF_6 is about three times higher than air. The insulation capability makes CF_3I a feasible alternative to SF_6 in a GIL system where arc quenching is not required. On the other hand, iodine deposition after every electrical discharge means CF_3I mixture may not be a suitable arc quenching gas for GIS applications that require high current interruption. However, the withstand tests on the RMU suggest CF_3I mixture may potentially be used in MV switchgear. The high boiling point of pure CF_3I means only low percentage of CF_3I content can be used in a gas mixture. More tests will be conducted on other CF_3I-CO_2 mixture ratios (20:80% and 10:90%) and CF_3I mixture with N_2 gas. This future work will be focussed on investigating CF_3I properties as an insulation medium.

Acknowledgements

This work was supported by Engineering and Physical Sciences Research Council (EPSRC), Transformation of the Top and Tail of Energy Networks Grant [grant number EP/I031707/1] and the IET Power Networks Research Academy.

BIBLIOGRAPHY

[1] H. Kasuya, H. Katagiri, Y. Kawamura, D. Saruhashi, and Y. Nakamura, "Measurement of Decomposed Gas Density of CF_3I-CO_2 Mixture", *16th International Symposium on High Voltage Engineering*, pp. 744-747, Cape Town, 2009.

[2] L. G. Christophorou and J. K. Olthoff, "Electron Interactions With CF_3I", *J. Phys. Chem.* , vol. 29, no. 4, pp. 553-569, 2000.

[3] Y. Y. Duan, M. S. Zhu, and L. Z. Han, "Experimental vapor pressure data and a vapor pressure equation for trifluoroiodomethane (CF_3I)", *Fluid Phase Equilibria*, vol. 121, pp. 227-234, 1996.

[4] G. J. M. Hagelaar and L. C. Pitchford, "Solving the Boltzmann equation to obtain electron transport coefficients and rate coefficients for fluid models", *Plasma Sources Science and Technology*, vol. 14, pp. 722-733, 2005.

[5] A. Haddad and D. Warne, "*Advances in High Voltage Engineering", IET Power series 41,*. London: The Institution of Engineering and Technology, 2004.

[6] T. Takeda, S. Matsuoka, A. Kumada, and K. Hidaka, "By-product Generation through Electrical Discharge in CF_3I Gas and its Effect to Insulation Characteristics", *IEEJ Transactions on Power and Energy*, vol. 131, no. 10, pp. 859-864, 2011.

[7] H. Katagiri, H. Kasuya, H. Mizoguchi, and S. Yanabu, "Investigation of the Performance of CF_3I Gas as a Possible Substitute for SF_6", *IEEE Trans. Dielectric Insulation*, vol. 15, no. 5, pp. 1424-1429, 2008.

[8] H. Kasuya, Y. Kawamura, H. Mizoguchi, Y. Nakamura, and S. Yanabu, "Interruption Capability and Decomposed Gas Density of CF_3I as a Substitute for SF_6 Gas", *IEEE Trans. Dielectric Electric Insulation*, vol. 17, pp. 1196-1203, 2010.

[9] T. Takeda, S. Matsuoka, A. Kumada, and K. Hidaka, "By-products of CF_3I produced by Spark Discharge", *10th Japan-Korea Joint Symposium on Electrical Discharge and High Voltage Engineering*, pp. 157-160, 2007.

[10] D. Kind and K. Feser, "*High-Voltage Test Techniques"*, 2nd ed. New Delhi: Shankar's Book Agency Pvt. Ltd. , 1999.

[11] L. B. Loeb and A. F. Kip, "Electrical Discharges in Air at Atmospheric Pressure - The Nature of the Positive and Negative Point-to-Plane Coronas and the Mechanism of Spark Propagation", *J. Appl. Phys.*, vol. 10, no. 3, pp. 142-160, 1939.

[12] C. N. Works and T. W. Dakin, "Dielectric Breakdown of Sulfur Hexalfluoride in Nonuniform Fields", *Transactions of American Institute of Electrical Engineers*, vol. 72, no. 5, pp. 682-689, 1953.

[13] B. S. BS62271-1, "High-voltage switchgear and controlgear - Part 1: Common specifications", British Standards Institution, 2008.

[14] CGIT Brochure 001, "Compressed Gas Insulated Transmission Bus Systems", 2004.

[15] E. Kuffel, W. S. Zaengl, and J. Kuffel, "*High Voltage Engineering - Fundamentals"*, 2nd ed. Butterworth-Heinemann, 2000.

[16] National Grid, "National Electricity Transmission System Security and Quality of Supply Standard Version 2.2", 2012.